Desalination and Water Treatment
www.deswater.com
doi: 10.5004/dwt.2021.27854

244 (2021) 167–179
December

Zeolite supported iron nanoparticles for the catalytic Fenton oxidative remediation of theophylline in aqueous medium

Mehwish Anis*, Sajjad Haydar

Institute of Environmental Engineering & Research (IEER), University of Engineering & Technology (UET), Lahore, Pakistan, Tel. +92 3214101534; email: mehwish@uet.edu.pk (M. Anis), Tel. +92 3004244868; email: sajjad@uet.edu.pk (S. Haydar)

Received 10 May 2021; Accepted 21 September 2021

ABSTRACT

Pharmaceutical active compounds (PhACs) are an emerging class of contaminants found in water and wastewater. The objective of this study was to develop and test a novel catalyst for the treatment of theophylline – a commonly occurring xanthine (a PhAC) for heterogeneous Fenton oxidation (HFO). The catalyst used was iron nanoparticle-loaded zeolite developed through coprecipitation of iron salts. Elemental composition, particle size and its distribution and Brunauer–Emmett–Teller surface area of the catalyst were determined. The deposition of iron nanoparticles was ensured through Fourier-transform infrared spectroscopy and X-ray diffraction techniques. Effect of treatment variables (pH, iron to oxidant ratio, and oxidation time) was evaluated through batch mode oxidation experiments. The experimental design was carved using response surface methodology and optimization done using Design-Expert v. 10.0 software. pH and iron to oxidant ratio were determined to be the most influencing parameters for theophylline removal. Moreover, it was observed that interaction between pH and iron to oxidant ratio, significantly affects the theophylline removal. Effective theophylline removal (~95%) was observed at pH 7, oxidation time of 60 min and iron to oxidant ratio of 3. Theophylline was transformed into its degradation product, that is, 1,3-methyluric acid after heterogeneous Fenton oxidation of theophylline. The developed catalyst was stable, durable and reusable for at least three experimental runs without compromising the catalyst performance. The treatment cost of theophylline using HFO was $14.41/m^3$.

Keywords: Theophylline; Heterogeneous Fenton oxidation; Design-Expert; Degradation products; Pharmaceutical active compounds

1. Introduction

Pharmaceutical active compounds (PhACs) are an emerging class of contaminants that enter the water and wastewater matrices from several sources [1]. The sources include the consumption and subsequent excretion of human and veterinary medicines, improper disposal of unused or expired medicines, effluents of pharmaceutical industries and hospitals, animal farms and feedlots, and effluents from wastewater treatment plants [2–4]. The presence of PhACs in significant concentrations has been reported in effluents from the pharmaceutical industry [5], municipal wastewater [6,7] and effluents from hospitals and medical centers [5,8,9].

PhACs even at very low concentrations affect aquatic life. Few impacts such as inhibition of the metabolic activity of living species, growth of antibiotic resilient microorganisms [10], abnormal changes in reproduction and development of zooplankton [11], and increased susceptibility of tadpoles to predation [12]. Fish are the most sensitive species to PhACs. The effects observed are: (1) changes in the behavior and feeding patterns, (2) accumulation of PhACs in the liver and brain tissues and cells [13–15], (3) increased activity and decreased sociability [16], (4) inhibition of enzymes and hormones and oxidative stress [17]. Ecotoxicological

* Corresponding author.

data are available for PhACs, however, most of the studies are based on a single compound. In actual wastewater, cocktails/mixture of these PhACs were found [18]. Hence, it may be expected that the actual effects of these PhACs would be deleterious than those predicted through these ecotoxicological studies [19].

PhACs generally escape the conventional treatment processes for wastewater, because these are not designed specifically for their treatment. Advanced oxidation processes (AOPs) have evolved as an effective treatment method for recalcitrant contaminants. The $OH^{\bullet}$ radicals, being the strongest oxidizing agents, mineralize the contaminants into carbon dioxide and water. AOPs such as photocatalysis, ozonation, Fenton process (homogeneous or heterogeneous), and wet air oxidation. Among these, the Fenton process has been extensively used for the treatment of many pharmaceuticals and personal care products (PPCPs). Fenton oxidation results in the production of hydroxyl radicals because of the reaction between H_2O_2 and Fe^{2+} under acidic conditions. The overall reaction between these two radicals can be represented through the following reaction:

$$H_2O_2 + Fe^{2+} \rightarrow Fe^{3+} + OH^{\bullet} + OH^{-} \quad (1)$$

$k = 63\ M^{-1}\ s^{-1}$

However, to produce hydroxyl radicals a chain of reactions is usually followed represented by the following reactions [20].

$$H_2O_2 + Fe^{3+} \rightarrow Fe^{2+} + OH_2^{\bullet} + H^{+} \quad (2)$$

$k = 1 \times 10^{-2}\ M^{-1}\ s^{-1}$

$$OH^{\bullet} + H_2O_2 \rightarrow HO_2 + H_2O \quad (3)$$

$k = 2.7 \times 10^{7}\ M^{-1}\ s^{-1}$

$$OH^{\bullet} + Fe^{2+} \rightarrow Fe^{3+} + OH^{-} \quad (4)$$

$k = 3.2 \times 10^{3}\ M^{-1}\ s^{-1}$

$$HO_2^{\bullet} + Fe^{3+} \rightarrow Fe^{2+} + O_2 + H^{+} \quad (5)$$

$k = 3.1 \times 10^{5}\ M^{-1}\ s^{-1}$

$$Fe^{2+} + HO_2^{\bullet} + H^{+} \rightarrow Fe^{3+} + H_2O_2 \quad (6)$$

$k = 1.2 \times 10^{6}\ M^{-1}\ s^{-1}$

$$HO_2^{\bullet} + HO_2^{\bullet} \rightarrow H_2O_2 + O_2 \quad (7)$$

$k = 8.3 \times 10^{5}\ M^{-1}\ s^{-1}$

$$HO_2^{\bullet} + H_2O_2 \rightarrow HO^{\bullet} + H_2O + O_2 \quad (8)$$

$k = 3\ M^{-1}\ s^{-1}$

However, ozonation and photocatalysis have evolved recently for the treatment of these PPCPs. Ozonation has been found as most effective method for the decontamination of many of the PhACs. A mixture of ibuprofen and clofibric acid was degraded up to 99% through ozone treatment [21]. Ozonation has been studied for the treatment of ibuprofen [21], diclofenac [22], paracetamol [23], naproxen and carbamazepine [24], erythromycin [25] and ofloxacin [26]. Although ozone has so far proved to be an effective treatment method for the PhACs, however, high energy consumption for ozone generation and provision of in-situ ozone generation owing to its short half-life limit the use of this process. Atenolol [27,28], amoxicillin and erythromycin [29], diclofenac [30], ibuprofen [31], clofibric acid [32,33] and bezafibrate [27] were studied for their decontamination through photocatalysis. Overall photocatalytic techniques were found effective for the treatment of PhACs. However, the major limitation is the energy requirements for the treatment process.

The recent focus has shifted to the hybrid approach of using different AOPs in combination with each other. Hybrid methods employed for treatment of PhACs are combinations of UV radiation and ozone with H_2O_2, TiO_2, Fe(II), and Fe(III) [34,35], photo-Fenton, solar photo-Fenton-like Fe(III)–EDDS complex [35], and several other combinations [36–38]. The addition of the second oxidation step resulted in rapid mineralization of the contaminants. However, the limitation to this hybrid approach is the higher costs involved [39].

Heterogeneous catalysis, although used for the treatment of PhACs, however, more focused remained on heterogeneous photocatalysis [40–43]. Little attention was paid to the heterogeneous catalytic Fenton process for the decontamination of wastewater from PhACs. In heterogeneous Fenton oxidation, the iron is deposited on support media like zeolites, clays, polymeric resins, and aluminates. Modified polyacrylonitrile was used for the removal of endocrine-disrupting compounds and some of the PPCPs [44]. Iron oxide nanoparticles were used as heterogeneous catalysts in the Fenton process for the treatment of paracetamol [45]. Iron-containing zeolite (Fe/MFI) was found effective in paracetamol degradation with total organic carbon removal of around 60% in 5 h [46]. Therefore, many opportunities exist to further explore the heterogeneous Fenton process for the treatment of this vast group of contaminants, that is, PhACs. The major advantages of heterogeneous Fenton oxidation include, wide operative pH range, no sludge formation and hence mitigation of associated cost issues [47].

The current study aimed to develop a novel catalyst for heterogeneous Fenton oxidation by depositing iron nanoparticles on a natural zeolite analcime for the treatment of PhACs. The PhACs targeted in this study were theophylline ($C_7H_8N_4O_2$). Theophylline belongs to the class of xanthine having a chemical composition of 1,3-dimethylxanthine commonly applied for the treatment of asthma. This xanthine derivative is prescribed to treat chronic obstructive pulmonary diseases. It is also used as a diuretic and cardiac and central nervous system stimulant. In addition, theophylline is a major constituent of black and green tea. The widespread use of this methylxanthine and its

occurrence, as a metabolite of caffeine, resulted in its presence in wastewater across the globe [48–50]. Hence, it was selected as the target contaminant.

The current study is useful for determining the effective treatment method for a pollutant that has wide occurrence belonging to the emerging class of contaminants. The novel catalyst prepared can further be used for the treatment studies of similar pollutants.

2. Materials and methods

2.1. Reagents

Analytical grade theophylline ($C_7H_8N_4O_2$) and sodium zeolite (analcime) having a chemical composition of ($Na_{16}Al_{16}Si_{32}O_{96}\cdot 16H_2O$) were purchased from Sigma-Aldrich (Singapore). For co-precipitation of iron nanoparticles, hexa-hydrated ferric chloride $FeCl_3\cdot 6H_2O$ and hepta-hydrated ferrous sulfate $FeSO_4\cdot 7H_2O$ were used. Hydrogen peroxide (H_2O_2) was used as an oxidant and purchased from Merck (Singapore). 0.1 N NaOH or H_2SO_4 were used for the pH adjustments whenever required.

2.2. Preparation of heterogeneous catalyst

Iron nanoparticles deposited ($Na_{16}Al_{16}Si_{32}O_{96}\cdot 16H_2O$) were prepared by the co-precipitation of $FeCl_3\cdot 6H_2O$ and $FeSO_4\cdot 7H_2O$. Appropriate quantities of aqueous solutions of $FeCl_3\cdot 6H_2O$ and $FeSO_4\cdot 7H_2O$ were heated together to 90°C on a hot plate. Then, to this mixture was added, 26% NH_3 solution. The NH_3 containing the mixture was then transferred instantaneously into zeolites solution and vigorously mixed together. The pH of the mixture was kept at 10. After 30 min of heating at 80°C, the mixture was then cooled to room temperature. Zeolites were separated from the solution through vacuum filtration. Black-colored iron nanoparticles were deposited onto zeolites. These were then washed with deionized water, dried and stored in an air-tight container for further use [51].

2.3. Characterization of a heterogeneous catalyst

Raw sodium zeolites and the prepared heterogeneous catalyst were analyzed for elemental composition through CHNSO Analyzer (4010 Costech ECS, USA) and atomic absorption spectrometer (400 PerkinElmer Analyst, USA). Litesizer 500 (Austria) was used to determine the particle size and its distribution of iron nanoparticles on raw sodium zeolite. Brunauer–Emmett–Teller quantachrome analyzer (NOVA 2200e, USA) was used to measure the specific surface area of the developed catalyst. Agilent Cary 630 FTIR spectrometer (USA) was used to determine the characteristic peaks of the elements present in the raw and prepared catalyst. X-ray diffraction peaks for both catalysts were obtained, employing powder diffractometer, at various 2θ values. The 2θ values ranged between 10° and 90°. The chemical nature of deposited Fe was estimated using the modified 1,10-phenanthroline method. In this method, the chemical nature of iron is estimated by quantifying iron (as total and as Fe^{2+}) [52].

2.4. Design of experiments

The effect of process parameters on the response is conventionally established by varying one-parameter-at-a-time (OPAT) while keeping all others constant in experimentation. Although widely used, the OPAT approach needs to be replaced with a statistically designed set of experiments. Design of experiments (DOE) is a statistical technique used for the systematic planning of experiments. The advantage of DOE over OPAT is that DOE enables the establishment of cause-effect relationship between the response and process parameters. Moreover, the interaction between various process parameters can also be identified through DOE which is not possible otherwise. DOE also identifies vital parameters which affect the process response. Furthermore, for achieving desired response, DOE aids in determining the optimized set of process parameters through numerical optimization. Lastly, DOE offers less number of experiments with reliable statistical analysis of the results as compared to the OPAT approach [53].

Given the benefits of DOE, the present study was designed based on a frequently used, user-defined, response surface methodology [54,55]. The software, Design-Expert v. 10.0 was used to design the experiments of heterogeneous Fenton oxidation of theophylline. The parameters that affect the oxidation included pH of the reaction (3,5,7), oxidation time (30, 45, 60 min) and Fe:H_2O_2 ratio (1,2,3). These were selected through screening experiments.

The DOE resulted in 27 experimental runs by varying combinations of different levels of the above-mentioned parameters. These experiments were conducted in triplicate and the corresponding average removal (response) of theophylline was noted (Table 1).

2.5. Experimental

1 g of theophylline was dissolved in 1,000 mL of deionized water to make a 1,000 mg L^{-1} stock solution. The stock solution was then further diluted to prepare standard solutions of; 10, 20, 30, 40, 50 and 100 mg L^{-1}. These solutions were analyzed through the high-performance liquid chromatography (HPLC) technique. HPLC with a UV detector (L-2420), of Hitachi Elite Gradient, was used for the analysis of theophylline. The column used was Inertsil ODS-3 (Dimensions: 4.6 mm × 250 mm). The mobile phase used for the detection of theophylline was methanol:water on a 60:40 v/v basis. The temperature and mobile phase flow rate employed to the column was 25°C and 0.75 mL min^{-1}, respectively.

2.5.1. Batch mode heterogeneous Fenton oxidation

Heterogeneous Fenton oxidation (HFO) of theophylline was carried out in batch mode. 100 mL of 100 mg L^{-1} of theophylline solution was taken in Erlenmeyer's glass reactors. The pH of the solution was adjusted as per DOE using 0.1 N NaOH and H_2SO_4.

An appropriate amount of prepared catalyst (2×10^{-3} M) was added to the glass reactor to maintain the iron concentration of 0.002 M. Hydrogen peroxide was then added, into the reactor, in the required quantity to maintain the

Fe:H_2O_2 ratio as per the suggested combinations (2×10^{-3} M, 4×10^{-3} M and 6×10^{-3} M for 1:1, 1:2 and 1:3 Fe:H_2O_2 ratio, respectively). The reaction mixture was agitated at 90 rpm for various oxidation times according to the DOE.

After designated oxidation time, the reaction was ceased by increasing the pH of the mixture to 10. This was done with the addition of 0.1 N NaOH. The reaction mixture was further heated in an oven for 10 min to eliminate excess H_2O_2. The catalyst was then recovered from the reaction mixture using 0.45 μm filter paper. The residual theophylline concentration was then determined using the HPLC technique. Several tests of quality assurance (QA) and quality control (QC) were performed during the analysis of theophylline using HPLC analysis. These include standard calibration, blank injection, precision and accuracy.

Catalyst stability is a vital parameter in the selection of catalysts. It was evaluated by determining the iron leaching from catalyst during treatment. The performance of the catalyst was evaluated based on its reusability in succeeding experiments under similar conditions. For this, the catalyst was reused for three successive runs, each of 60 min, for the removal of theophylline.

Table 1
Experimental combinations and respective removal of theophylline

Run no.	pH	Oxidation time (min)	Fe:H_2O_2 ratio	Removal (%)
1	5	30	3	91
2	7	45	2	83
3	5	30	1	73
4	7	45	3	96
5	7	30	2	89
6	5	45	2	87
7	3	60	2	98
8	7	60	3	97
9	5	60	1	72
10	3	30	1	74
11	3	45	2	99
12	7	30	3	92
13	7	60	1	81
14	7	60	2	93
15	3	60	1	99
16	7	30	1	74
17	3	45	3	96
18	3	60	3	100
19	3	45	1	99
20	5	60	3	82
21	5	30	2	94
22	7	45	1	74
23	3	30	3	99
24	5	45	3	100
25	3	30	2	98
26	5	60	2	88
27	5	45	1	76

2.5.2. Fate of theophylline in HFO

Standard solutions of 10 mg L^{-1} of theophylline and its probable degradation products were prepared. These were then analyzed through a UV spectrophotometer. The analytical wavelength ranged from 400–700 nm. The peaks of each compound were identified corresponding to their respective lambda max (λ_{max}). The range of analysis was narrowed down depending on the presence of specific peaks. Afterward, the parent compounds and the degradation products were mixed and analyzed within a narrower wavelength. The respective peaks of parent compounds and degradation products in the mixture were noted.

The treated theophylline solutions after optimized HFO were then analyzed within the reduced wavelength range. Peaks of each compound were identified at their respective λ_{max} and their absorbance was noted. The respective concentration of each compound was then determined proportionally to the absorbance of standard peaks of these compounds in a mixture. This indicated the type and quantity of the degradation product formed after the heterogeneous oxidation of theophylline.

2.6. Data analysis

Results obtained from experimental runs were fitted to various regression models. The best-fitted model was selected based on its statistical adequacy determined by analysis of variance (ANOVA). The selected model was further employed to study the effect of process variables and their interaction on the removal of theophylline. Significant terms of the selected model were identified using ANOVA results. Process parameters were optimized to obtain the optimal conditions for the removal of theophylline.

3. Results and discussion

3.1. Characterization of the prepared catalyst

The elemental composition of raw and modified zeolites is presented in Table 2.

The size of iron nanoparticles ranged from 40.5 to 85 nm with a mean particle size of 60 nm. The size of particles was observed to lie between 1–100 nm, hence considered as nanoparticles. The specific area of the catalyst, after deposition of iron nanoparticles, was noted to be 20.65 g m^{-2}. Using the modified 1,10-phenanthroline method, it was

Table 2
Elemental composition of raw and modified zeolites

Element	Proportion (%)	
	Raw zeolites	Iron-deposited zeolites
Na	10.44	7.15
Al	12.26	8.4
Si	25.51	17.47
H	0.92	0.63
O	50.87	34.84
Fe	Nil	31.5

revealed that the iron species were deposited on the catalyst in Fe^{2+}/Fe^{3+} ratio of 0.35 ± 0.05.

The Fourier-transform infrared spectroscopy (FTIR) of zeolites, both raw and iron-deposited, are shown in Fig. 1a and b. Peaks of Si–O stretching were indicated in the spectrum of raw zeolites at 1,171 and 1,121 cm^{-1} (Fig. 1a). Similarly, the characteristic peaks of sodium aluminosilicate zeolite were represented by the peak of Al–(O) at 832 cm^{-1} and that of (O)–Na–(O) at 1,036 cm^{-1}. The additional peaks at 1,632 cm^{-1} (–OH bonding) and 3,423 cm^{-1} (–C=O) could be due to the polymer added in the synthetic zeolite. The spectrum of iron-loaded zeolites (Fig. 1b) denotes comparable forms of peaks like that of raw zeolites, with an extra peak at 668 cm^{-1}, of Fe–(O). This additional peak represents the effective deposition of iron on zeolites.

The characterization of zeolites was also performed using the X-ray diffraction (XRD) technique and the resulting patterns are shown in Fig. 2a and b. The typical diffraction peak of sodium aluminosilicate is indicated in Fig. 2a at 2θ values of 15.8°, 25.9° and 30.5°. In the XRD pattern of iron-loaded zeolites, two additional peaks were shown at 2θ of 43° and 45.5° (Fig. 2b). These peaks represent the presence of Fe–O–Al and (Fe–O–Si), respectively.

The conclusions of XRD patterns agreed with the results obtained by FTIR spectra, both signifying the successful iron deposition onto zeolites. The distribution of iron as Fe^{2+} and Fe^{3+} adhered on the zeolites in form of nanoparticles was determined, as discussed in section 2.3. This distribution is represented as a ratio of Fe^{2+} to Fe^{3+}, which came out to be 0.35 ± 0.05.

3.2. Regression analysis

It can be observed in Table 1, that the theophylline removal ranged from 72% to 100% with an average removal of 89%. The theophylline removal data were then fitted to the regression analysis to determine the best fit model equation. Among various models, quadratic was found to

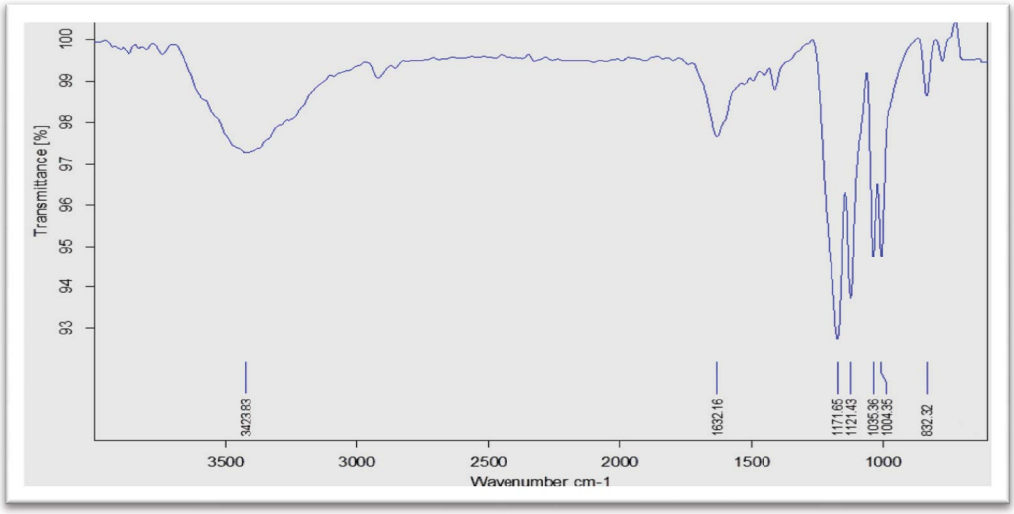

(a)

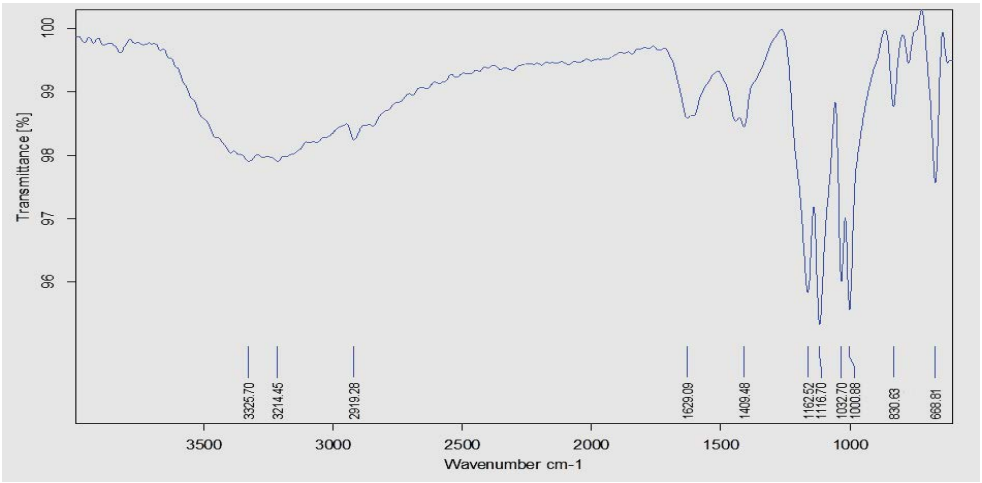

(b)

Fig. 1. Fourier-transform infrared spectroscopy of raw and modified catalyst. (a) Raw zeolites and (b) Modified zeolites (Iron deposited).

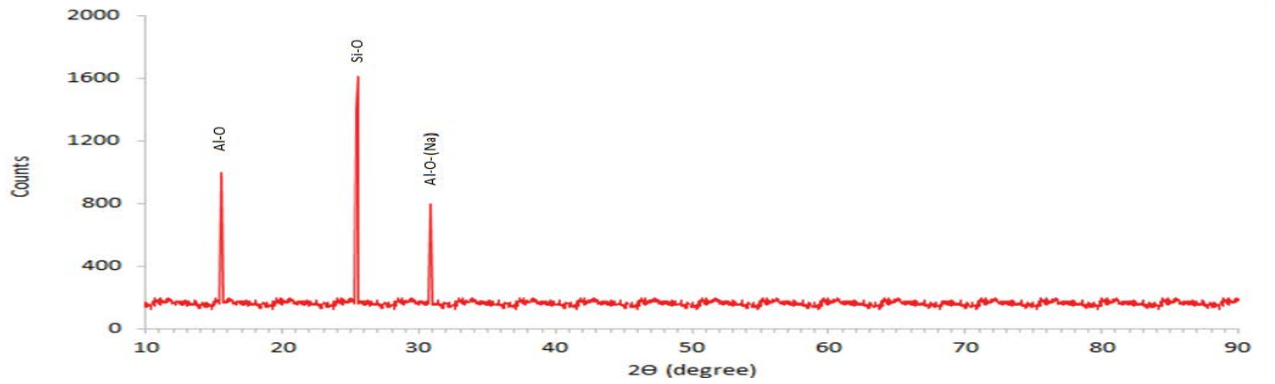

(a)

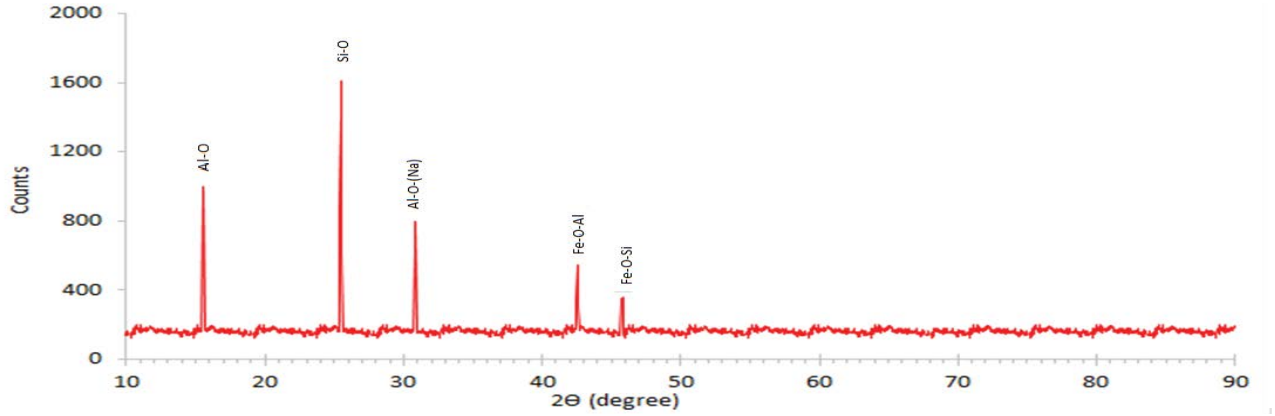

(b)

Fig. 2. X-ray diffraction results for raw and modified catalyst. (a) Raw zeolites and (b) Modified (iron deposited) zeolites.

be the best in representing theophylline removal through HFO. Selection of the most suitable model was based on *p*-value (for quadratic model 0.03 < 0.05), the lowest standard deviation of 5.98 and lowest predicted residual error of sum of squares (PRESS) of 1,662 with a regression coefficient of 0.76, for the quadratic model.

The quadratic model initially fitted to the removal of theophylline in terms of the coded factors given in Eq. (9).

$$\text{R.E.} = 88.81 - 4.61A + 1.44B + 7.28C - 0.83AB + 2.75AC - 2.83BC + 6.39A^2 + 1.44B^2 - 4.61C^2 \quad (9)$$

where A = pH; B = oxidation time (min); C = Fe:H_2O_2 ratio.

3.3. Analysis of variance

The significance of the quadratic model was determined through ANOVA. The results for the response surface quadratic model fitted to the HFO of theophylline are presented in Table 3.

The model *p*-value of 0.0007 < 0.05 indicated that there are only 0.07% chances that the results obtained are by chance. Moreover, the *F*-value of 6.06 is greater than $F_{critical}$ of 2.49 which implied that the model is significant.

Based on Prob. > *F* values, the significant model terms were identified. The terms A (pH), C (Fe:H_2O_2) have a *p*-value < 0.05, hence are the significant terms of the model. Similarly, quadratic terms of these parameters (A^2 and C^2) also have *p*-value < 0.05 indicating their significance. The *p*-value (0.0751 > 0.05) of B (contact time) indicated that it is relatively less significant than the pH and Fe:H_2O_2 ratio for the theophylline removal. The influential parameters for theophylline were also determined by estimating their percentage contribution in the removal using the following equation.

$$\%\ \text{Contribution} = \frac{\text{mean square of each factor}}{\text{sum of mean squares of all factors}} \quad (10)$$

The results are presented in the form of a Pareto chart [56] as shown in Fig. 3.

It is evident from Fig. 3 that Fe:H_2O_2 was the most influential factor (48.79%) affecting the oxidation of theophylline. pH also showed a significant (19.59%) contribution in theophylline removal. The higher-order terms of these two parameters also contributed significantly to theophylline removal. The rest of the parameters did not contribute considerably.

Table 3
ANOVA for results of selected model (quadratic) for theophylline

Source	Sum of squares	Degree of freedom, df	Mean square	*F*-value	*p*-value Prob. > *F*
Model	1,954.08	9	217.12	6.06	0.0007
A-pH	382.72	1	382.72	10.69	0.0045
B-contact time	37.56	1	37.56	1.05	0.0751
C-Fe:H_2O_2	953.39	1	953.39	26.62	<0.0001
AB	8.33	1	8.33	0.23	0.6357
AC	90.75	1	90.75	2.53	0.0999
BC	96.33	1	96.33	2.69	0.1194
A^2	244.91	1	244.91	6.84	0.0181
B^2	12.52	1	12.52	0.35	0.5622
C^2	127.57	1	127.57	3.56	0.0463
Residual	608.88	17	35.82		
Cor. total	2,562.96	26			

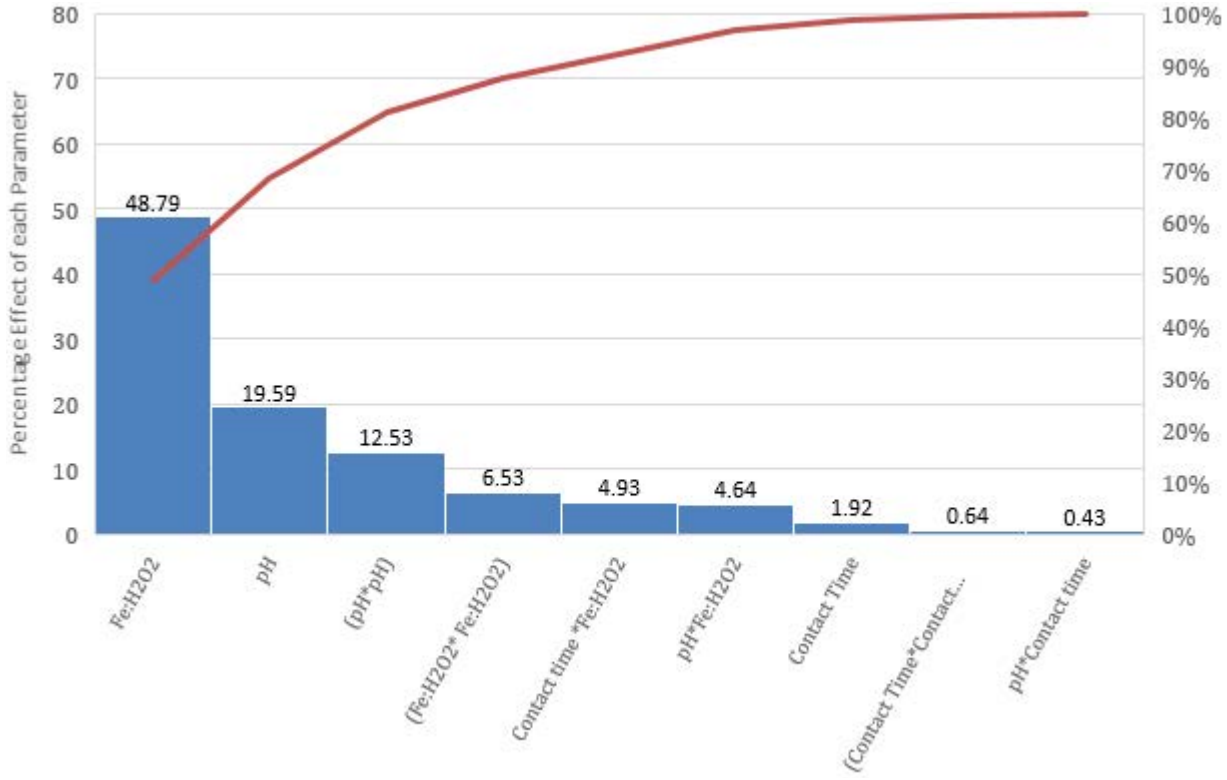

Fig. 3. Pareto chart showing the effect of parameters on the removal of theophylline.

3.4. Interaction among process factors

The regression Eq. (9) suggested that interaction of pH and Fe:H_2O_2 ratio also influence the theophylline removal in addition to pH and Fe:H_2O_2 ratio. The contour plots are shown in Fig. 4 shed light on the interaction between the above-stated parameters.

The elliptical contour lines indicate the presence of interaction among pH and Fe:H_2O_2 ratio. Contour plots at a contact time of 30 min (Fig. 4a) suggested that removal greater than 95% (orange shaded region) can be achieved within a narrow pH of 3–3.2 with Fe:H_2O_2 ratio ranging from 1.3–3. However, significant removal from 80%–90% can be achieved at a wide range of pH and Fe:H_2O_2 ratio (blue shaded region).

A similar pattern can be observed when the contact time was increased from 30–45 min. In addition, orange shaded region indicating >95% removal started appearing at pH 7 and Fe:H_2O_2 ratio of 2.5–3. This region became prominent when the contact time was further increased to 60 min. This indicated that the acidic pH required for the

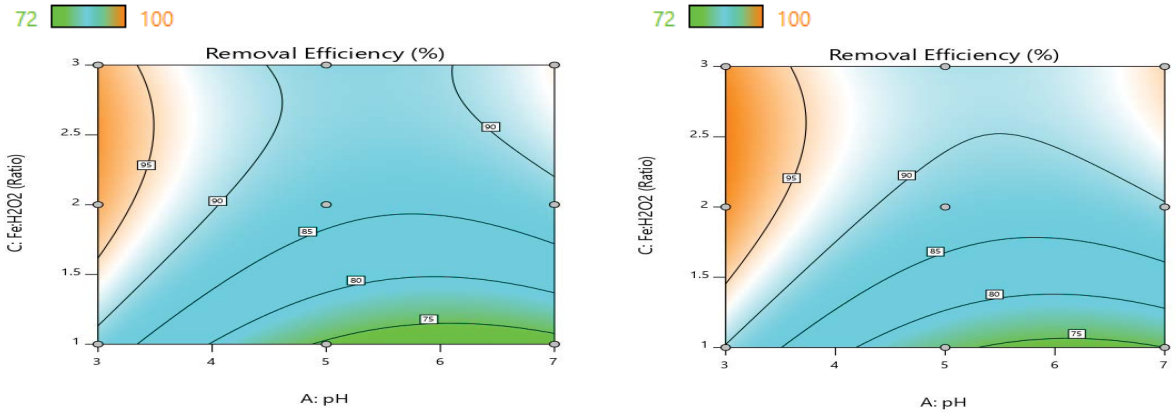

(a) pH vs Fe:H_2O_2ratio
contact time = 30 min

(b) pH vs Fe:H_2O_2ratio
contact time = 45 min

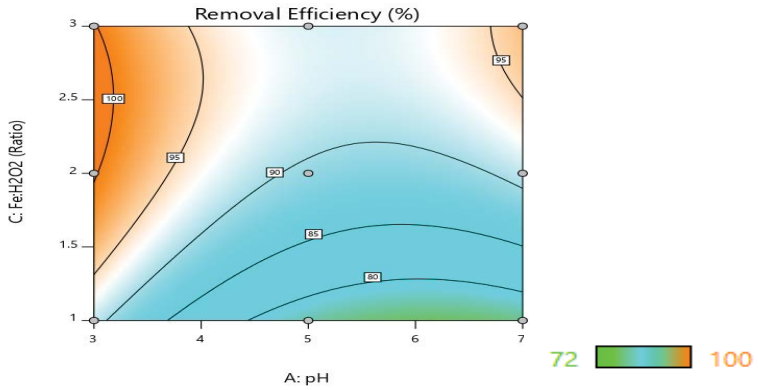

(c) pH vs Fe:H_2O_2ratio
contact time = 60 min

Fig. 4. Contour plots for heterogeneous Fenton oxidation of theophylline.

homogeneous Fenton process can be avoided in HFO if the contact time and Fe:H_2O_2 ratio is increased to 60 min and 2.5–3.0, respectively.

The homogeneous Fenton reactions are favored under acidic pH as iron precipitate outs as $Fe(OH)_3$ sludge at pH > 4. However, this limitation was not present for HFO (Fig. 4), where better removal was achieved even at around neutral pH. This is a key benefit of the heterogeneous Fenton process. This can be attributed to the availability of Fe^{2+} catalyst in active form in HFO at or near neutral pH rather than in the form of $Fe(OH)_3$ sludge in homogeneous Fenton oxidation.

3.5. Numerical optimization

Numerical optimization was carried to determine the optimal settings of the process parameters based on the desirability function. It furnished the combinations of treatment variables that could attain desired output levels (removal) with a specified range of input parameters.

The criteria for pH, contact time and Fe:H_2O_2 ratio was set to be "within range" whereas the removal of theophylline was "maximized" to achieve maximal oxidation of theophylline. These criteria were combined into a single desirability function which was then maximized by the Design-Expert 10.0 to achieve the optimal parameter settings for the removal of theophylline through HFO. The graphical view of the numerical optimization is shown in Fig. 5.

Theophylline removal up to 95% is expected at optimized pH of 7, 60 min contact time, and Fe:H_2O_2 ratio of 3. The desirability of 0.753 indicated the favorability of the solution.

3.6. Degradation products of theophylline

The potential persistent degradation products of theophylline along with their λ_{max} and corresponding absorbance for 10 mg L^{-1} solution are shown in Table 4.

Theophylline is converted into various degradation products during its mineralization into CO_2 and H_2O. However, not all degradation products persisted after the completion of heterogeneous oxidation. The degradation products that lasted even after the completion of heterogeneous oxidation are shown in UV spectra in Fig. 5.

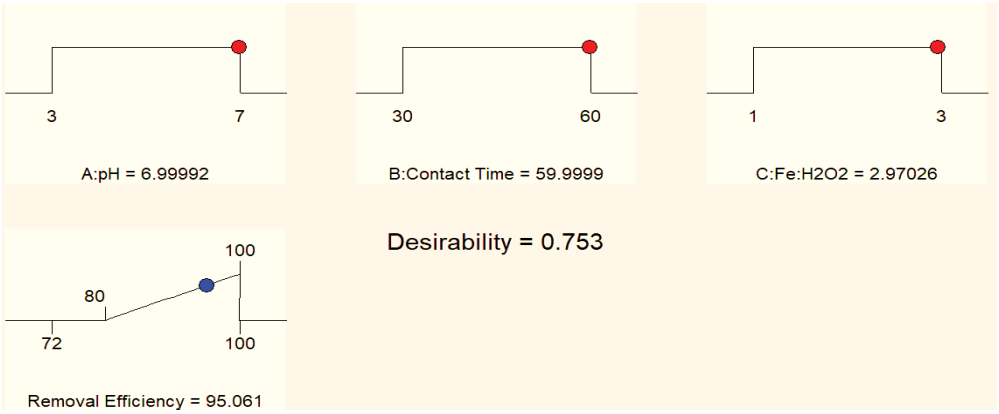

Fig. 5. Numerical optimization ramps for heterogeneous Fenton oxidation of theophylline.

Table 4
λ_{max} and absorbance of degradation products of theophylline

Sr. no.	Degradation product	λ_{max} (nm)	Maximum absorbance
1.	1-Methyluric acid	231,284	2.59
2.	1,3-Dimethyluric acid	231,287	1.63

Two distinct peaks are observed in Fig. 6. The peak-1 at 231 nm was characteristic of derivatives of uric acid while the peak-2 at 284 nm indicated the presence of 1-methyluric acid. The concentration of 1-methyluric acid corresponding to peak-2 was 8.72 mg L^{-1}. This indicated 87% mineralization of theophylline into simpler products including CO_2 and water.

3.6.1. Proposed mechanism for the conversion of theophylline to degradation products

Degradation of theophylline into persistent compounds showed that it underwent a series of reactions that resulted in by-products. It may be presumed that hydroxyl radical initiated the oxidation process through hydroxylation in which the C–H bond is broken by OH radicals and converted into C–O–H bond. Further hydroxyl radical abstracted the hydrogen atom and converted initially into 1,3-dimethyluric acid; which was unstable. Therefore, undergone demethylation, that is, removal of methyl ($–CH_3$) group and converted into 1-methyluric acid as shown in Fig. 7. 1,3-dimethyluric acid was observed to persist even after oxidation of theophylline.

4. Catalyst stability and performance

The presence of iron was examined in the filtrate of treated theophylline samples. Leaching of iron was detected in only one out of five samples in which iron concentration was 0.013 mg L^{-1}. In the rest of the analyzed samples, iron concentration was less than the detection limit (i.e., 0.0005 mg L^{-1}). This indicated the stability of the prepared catalyst which did not leach out in the treated sample. Hence the experimental conditions sustained the heterogeneity of the reaction.

Along with leaching, the reusability of the catalyst is another key indicator of its performance. To assess its reusability potential, the catalyst was reused in 3 successive batches, each of 60 min, for the removal of theophylline. The removal of theophylline observed was 97.7%, 96.8% and 96.9% in the first, second, and third run, respectively. The removal of theophylline in three successive batches is shown in Fig. 8.

A good average removal was obtained (i.e., 95.8% + 0.709%). The reusability of catalyst is evident in at least 3 successive runs, each of 60 min, without significant loss in catalyst activity.

5. Cost analysis

Cost is one of the deciding parameters in the selection of the treatment process. Hence, cost estimation is relevant. In this study cost calculations such as (1) synthetic zeolites, (2) pH adjustment, (3) deposition of iron nanoparticles and (4) oxidant. Table 5 presents the treatment cost per m^3 of water for the novel catalyst.

As shown in Table 5, per m^3 cost for treatment theophylline through HFO was $14.41. The treatment cost is quite less as compared to the cost of treatment for other pollutants treated through homogeneous Fenton oxidation, that is, $43.4/$m^3$ for butyric acid, $88.1/$m^3$ for propanol and $57.1/$m^3$ for Eriochrome black T [57].

6. Conclusions

The zeolite-supported iron nanoparticles were found effective for the treatment of theophylline from aqueous solutions. More than 95% removal of theophylline was observed at neutral pH of 7 with high iron to oxidant ratio and contact time. Theophylline removal was not linear with respect to the process parameters. Interaction among the process parameters including pH and Fe:H_2O_2 ratio was observed to be present and significantly affecting the removal of theophylline. HFO did not result in the complete mineralization of theophylline into carbon dioxide and water. It was found to transform into

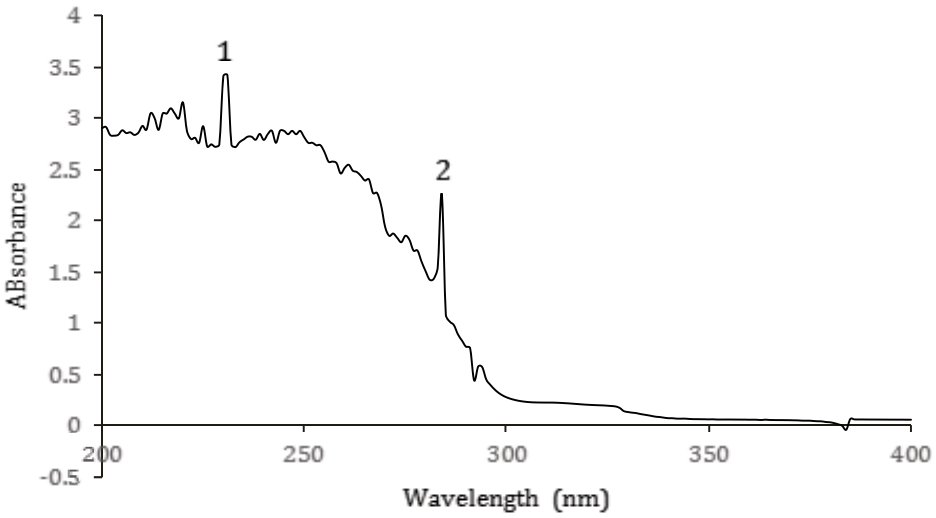

Fig. 6. UV spectra for the identification of degradation products of theophylline.

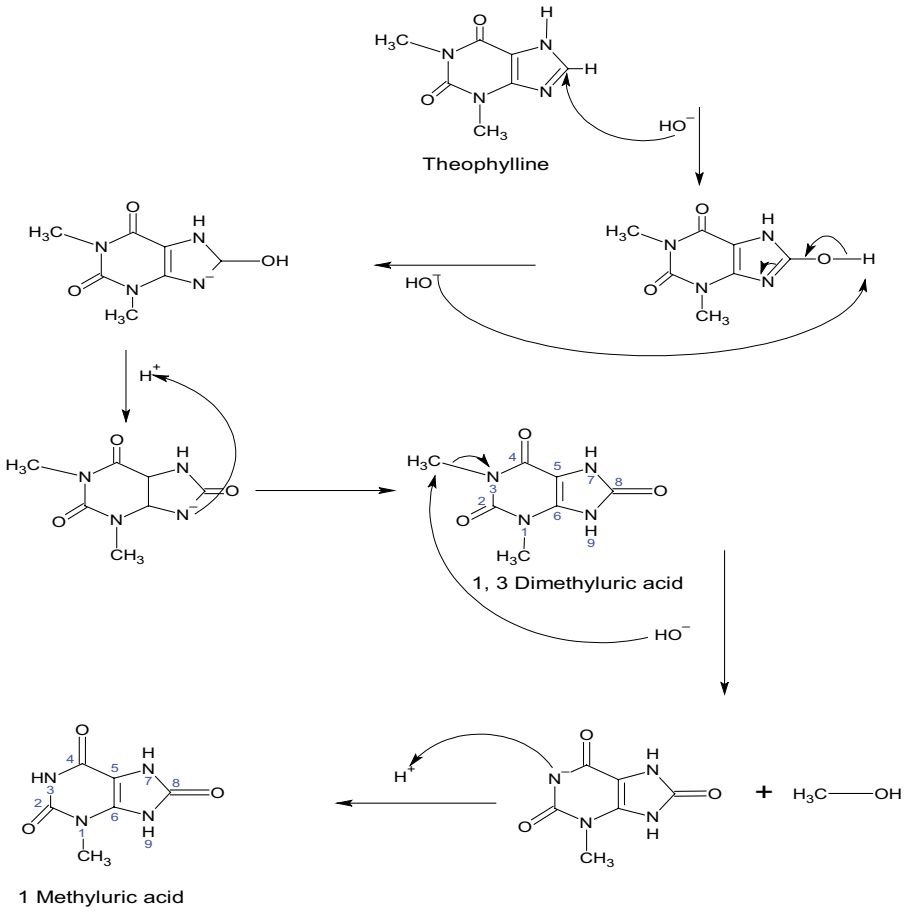

Fig. 7. Proposed mechanism for the conversion of theophylline into its degradation products.

1,3-dimethyluric acid, though in low (8.72 mg L^{-1}) but persistent concentration. The cost of HFO of theophylline was estimated to be \$14.41/m^3. The prepared catalyst was found stable and durable and can be reused for at least 3 successive runs. Since the current study was carried out in batch mode at a laboratory scale, these optimized parameters can initially be used for conducting pilot-scale studies.

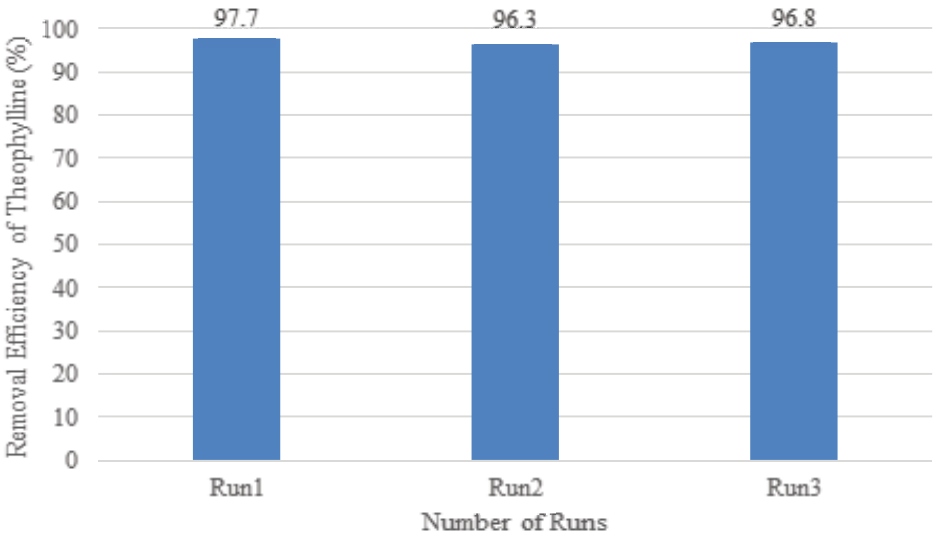

Fig. 8. Removal of theophylline in multiple runs.

Table 5
Cost of heterogeneous Fenton oxidation of theophylline

	Quantity consumed (kg)	Unit cost ($/kg)	Total cost ($)
Cost of preparation of 1 kg catalyst			
Zeolites	0.66	57.20	37.75
$FeSO_4 \cdot 6H_2O$	0.28	35.20	9.85
$FeCl_3 \cdot 7H_2O$	0.40	33.40	13.56
Total cost			61.17
Cost of treatment of 1 m^3 water			
	Quantity consumed (kg m^{-3})	Unit cost ($/kg)	Total cost ($/$m^3$)
Prepared catalyst	0.25	61.17	12.23
H_2O_2	0.10	21.88	2.18
Total cost			14.41

7. Funding sources

This research did not receive any specific grant from funding agencies in the public, commercial, or not-for-profit sectors.

References

[1] B. Petrie, R. Barden, B. Kasprzyk-Hordern, A review on emerging contaminants in wastewaters and the environment: current knowledge, understudied areas and recommendations for future monitoring, Water Res., 72 (2015) 3–27.
[2] A. Nikolaou, S. Meric, D. Fatta, Occurrence patterns of pharmaceuticals in water and wastewater environments, Anal. Bioanal. Chem., 387 (2007) 1225–1234.
[3] S. Gaw, K.V. Thomas, T.H. Hutchinson, Sources, impacts and trends of pharmaceuticals in the marine and coastal environment, Philos. Trans. R. Soc. London, Ser. B, 369 (2014) 2013.0572, doi: 10.1098/rstb.2013.0572.
[4] J.F. Narvaez, C. Jimenez, Pharmaceutical products in the environment: sources, effects and risks, Vitae, 19 (2012) 93–108.
[5] W.-J. Sim, J.-W. Lee, E.-S. Lee, S.-K. Shin, S.-R. Hwang, J.-E. Oh, Occurrence and distribution of pharmaceuticals in wastewater from households, livestock farms, hospitals and pharmaceutical manufactures, Chemosphere, 82 (2011) 179–186.
[6] N. Collado, S. Rodriguez-Mozaz, M. Gros, A. Rubirola, D. Barceló, J. Comas, I. Rodriguez-Roda, G. Buttiglieri, Pharmaceuticals occurrence in a WWTP with significant industrial contribution and its input into the river system, Environ. Pollut., 185 (2014) 202–212.
[7] P. Verlicchi, M. Al Aukidy, E. Zambello, Occurrence of pharmaceutical compounds in urban wastewater: removal, mass load and environmental risk after a secondary treatment—a review, Sci. Total Environ., 429 (2012) 123–155.
[8] O. Frédéric, P. Yves, Pharmaceuticals in hospital wastewater: their ecotoxicity and contribution to the environmental hazard of the effluent, Chemosphere, 115 (2014) 31–39.
[9] T.S. Oliveira, M. Murphy, N. Mendola, V. Wong, D. Carlson, L. Waring, Characterization of Pharmaceuticals and Personal Care products in hospital effluent and waste water influent/effluent by direct-injection LC-MS-MS, Sci. Total Environ., 518–519 (2015) 459–478.
[10] S. Aydin, B. Ince, O. Ince, Development of antibiotic resistance genes in microbial communities during long-term operation of anaerobic reactors in the treatment of pharmaceutical wastewater, Water Res., 83 (2015) 337–344.

[11] C.M. Flaherty, S.I. Dodson, Effects of pharmaceuticals on Daphnia survival, growth, and reproduction. Chemosphere, 61 (2005) 200–207.
[12] D.E. Conners, E.D. Rogers, K.L. Armbrust, J.-W. Kwon, M.C. Black, Growth and development of tadpoles (*Xenopus laevis*) exposed to selective serotonin reuptake inhibitors, fluoxetine and sertraline, throughout metamorphosis, Environ. Toxicol. Chem., 28 (2009) 2671–2676.
[13] B.W. Brooks, C. Kevin Chambliss, J.K. Stanley, A. Ramirez, K.E. Banks, R.D. Johnson, R.J. Lewis, Determination of select antidepressants in fish from an effluent-dominated stream, Environ. Toxicol. Chem., 24 (2005) 464–469.
[14] J. Corcoran, M.J. Winter, C.R. Tyler, Pharmaceuticals in the aquatic environment: a critical review of the evidence for health effects in fish, Crit. Rev. Toxicol., 40 (2010) 287–304.
[15] A. Harada, K. Komori, N. Nakada, K. Kitamura, Y. Suzuki, Biological effects of PPCPs on aquatic lives and evaluation of river waters affected by different wastewater treatment levels, Water Sci. Technol., 58 (2008) 1541–1546.
[16] T. Brodin, J. Fick, M. Jonsson, J. Klaminder, Dilute concentrations of a psychiatric drug alter behavior of fish from natural populations, Science, 339 (2013) 814–815.
[17] E.J. Zillioux, I.C. Johnson, Y. Kiparissis, C.D. Metcalfe, J.V. Wheat, S.G. Ward, H. Liu, The sheepshead minnow as an in vivo model for endocrine disruption in marine teleosts: a partial life-cycle test with 17α-ethynylestradiol, Environ. Toxicol. Chem., 20 (2001) 1968–1978.
[18] P.H. Roberts, K.V. Thomas, The occurrence of selected pharmaceuticals in wastewater effluent and surface waters of the lower Tyne catchment, Sci. Total Environ., 356 (2006) 143–153.
[19] L. Cizmas, V.K. Sharma, C.M. Gray, T.J. McDonald, Pharmaceuticals and personal care products in waters: occurrence, toxicity, and risk, Environ. Chem. Lett., 13 (2015) 381–394.
[20] A.G. Gutierrez-Mata, S. Velazquez-Martínez, A. Álvarez-Gallegos, M. Ahmadi, J.A. Hernández-Pérez, F. Ghanbari, S. Silva-Martínez, Recent overview of solar photocatalysis and solar photo-Fenton processes for wastewater treatment, Int. J. Photoenergy, 2017 (2017) 8528063, doi: 10.1155/2017/8528063.
[21] M. Quero-Pastor, A. Valenzuela, J.M. Quiroga, A. Acevedo, Degradation of drugs in water with advanced oxidation processes and ozone, J. Environ. Manage., 137 (2014) 197–203.
[22] F.J. Beltrán, P. Pocostales, P. Alvarez, A. Oropesa, Diclofenac removal from water with ozone and activated carbon, J. Hazard. Mater., 163 (2009) 768–776.
[23] M. Neamțu, M. Bobu, A. Kettrup, I. Siminiceanu, Ozone photolysis of paracetamol in aqueous solution, J. Environ. Sci. Health. Part A Toxic/Hazard. Subst. Environ. Eng., 48 (2013)1264–1271.
[24] R. Rosal, A. Rodríguez, M.S. Gonzalo, E. García-Calvo, Catalytic ozonation of naproxen and carbamazepine on titanium dioxide, Appl. Catal., B, 84 (2008) 48–57.
[25] D.B. Luiz, A.K. Genena, E. Virmond, H.J. José, R.F.P.M. Moreira, W. Gebhardt, H. Fr Schröder, H, Identification of degradation products of erythromycin A arising from ozone and advanced oxidation process treatment, Water Environ. Res., 82 (2010) 797–805.
[26] J.B. Carbajo, A.L. Petre, R. Rosal, S. Herrera, P. Letón, E. García-Calvo, A.R. Fernández-Alba, J.A. Perdigón-Melón, Continuous ozonation treatment of ofloxacin: transformation products, water matrix effect and aquatic toxicity, J. Hazard. Mater., 292 (2015) 34–43.
[27] N. De la Cruz, J. Giménez, S. Esplugas, D. Grandjean, L.F. de Alencastro, C. Pulgarín, Degradation of 32 emergent contaminants by UV and neutral photo-Fenton in domestic wastewater effluent previously treated by activated sludge, Water Res., 46 (2012) 1947–1957.
[28] F.L. Rosario-Ortiz, E.C. Wert, S.A. Snyder, Evaluation of UV/H_2O_2 treatment for the oxidation of pharmaceuticals in wastewater, Water Res., 44 (2010) 1440–1448.
[29] R. Sharmin, S.J. Chowdhury, A review on the removal of pharmaceuticals and personal care products from wastewater, Int. J. Sci. Res., 5 (2016) 33–35.
[30] D. Vogna, R. Marotta, A. Napolitano, R. Andreozzi, M. d'Ischia, M., Advanced oxidation of the pharmaceutical drug diclofenac with UV/H_2O_2 and ozone, Water Res., 38 (2004) 414–422.
[31] F. Méndez-Arriaga, S. Esplugas, J. Giménez, Degradation of the emerging contaminant ibuprofen in water by photo-Fenton, Water Res., 44 (2010) 589–595.
[32] R. Andreozzi, V. Caprio, R. Marotta, A. Radovnikovic, Ozonation and H_2O_2/UV treatment of clofibric acid in water: a kinetic investigation, J. Hazard. Mater., 103 (2003) 233–246.
[33] R.R. Giri, H. Ozaki, S. Ota, R. Takanami, S. Taniguchi, Degradation of common pharmaceuticals and personal care products in mixed solutions by advanced oxidation techniques, Int. J. Environ. Sci. Technol., 7 (2010) 251–260.
[34] F. Javier Benitez, J.L. Acero, F.J. Real, G. Roldan, F. Casas, Comparison of different chemical oxidation treatments for the removal of selected pharmaceuticals in water matrices, Chem. Eng. J., 168 (2011) 1149–1156.
[35] S. Miralles-Cuevas, F. Audino, I. Oller, R. Sánchez-Moreno, J.A. Sánchez Pérez, S. Malato, Pharmaceuticals removal from natural water by nanofiltration combined with advanced tertiary treatments (solar photo-Fenton, photo-Fenton-like Fe(III)–EDDS complex and ozonation), Sep. Purif. Technol., 122 (2014) 515–522.
[36] Y. Lester, D. Avisar, I. Gozlan, H. Mamane, Removal of pharmaceuticals using combination of UV/H_2O_2/O_3 advanced oxidation process, Water Sci. Technol., 64 (2011) 2230–2238.
[37] S. Chelliapan, P.J. Sallis, Removal of organic compound from pharmaceutical wastewater using advanced oxidation processes, J. Sci. Ind. Res., 72 (2013) 248–254.
[38] A. Cesaro, V. Belgiorno, Removal of endocrine disruptors from urban wastewater by advanced oxidation processes (AOPs): a review, Open Biotechnol. J., 10 (2016) 151–172.
[39] A. Morone, P. Mulay, S.P. Kamble, Chapter 8 – Removal of Pharmaceutical and Personal Care Products from Wastewater Using Advanced Materials, M.N. Vara Prasad, M. Vithanage, A. Kapley, Eds., Pharmaceuticals and Personal Care Products: Waste Management and Treatment Technology: Emerging Contaminants and Micro Pollutants, Butterworth-Heinemann, Elsevier, India, 2019, pp. 173–212.
[40] R. Liang, A. Hu, W. Li, Y.N. Zhou, Enhanced degradation of persistent pharmaceuticals found in wastewater treatment effluents using TiO_2 nanobelt photocatalysts, J. Nanopart. Res., 15 (2013) 1–13, doi: 10.1007/s11051-013-1990-x.
[41] A. Kaur, A. Umar, S.K. Kansal, Heterogeneous photocatalytic studies of analgesic and non-steroidal anti-inflammatory drugs, Appl. Catal., A, 510 (2016) 134–155.
[42] P. Soriano-Molina, P. Plaza-Bolaños, A. Lorenzo, A. Agüera, J.L. García Sánchez, S. Malato, J.A. Sánchez Pérez, Assessment of solar raceway pond reactors for removal of contaminants of emerging concern by photo-Fenton at circumneutral pH from very different municipal wastewater effluents, Chem. Eng. J., 366 (2019) 141–149.
[43] J.L. Rodríguez-Gil, M. Catalá, S.G. Alonso, R.R. Maroto, Y. Valcárcel, Y. Segura, R. Molina, J.A. Melero, F. Martínez, Heterogeneous photo-Fenton treatment for the reduction of pharmaceutical contamination in Madrid Rivers and ecotoxicological evaluation by a miniaturized fern spores bioassay, Chemosphere, 80 (2010) 381–388.
[44] G.T. Chi, J. Churchley, K.D. Huddersman, Pilot-scale removal of trace steroid hormones and pharmaceuticals and personal care products from municipal wastewater using a heterogeneous Fenton's catalytic process, Int. J. Chem. Eng., 2013 (2013) 760915, doi: 10.1155/2013/760915.
[45] C. Velichkova, C. Julcour-Lebigue, B. Koumanova, H. Delmas, Heterogeneous Fenton oxidation of paracetamol using iron oxide (nano)particles, J. Environ. Chem. Eng., 1 (2013) 1214–1222.
[46] F. Velichkova, H. Delmas, C. Julcour, B. Koumanova, Heterogeneous Fenton and photo-Fenton oxidation for

paracetamol removal using iron containing ZSM-5 zeolite as catalyst, AIChE J., 63 (2017) 669–679.
[47] J.P. Ribeiro, M.I. Nunes, Recent trends and developments in Fenton processes for industrial wastewater treatment – a critical review, Environ. Res., 197 (2021) 110957, doi: 10.1016/j.envres.2021.110957.
[48] T. Okuda, N. Yamashita, H. Tanaka, H. Matsukawa, K. Tanabe, Development of extraction method of pharmaceuticals and their occurrences found in Japanese wastewater treatment plants, Environ. Int., 35 (2009) 815–820.
[49] J.W. Kim, S.M. Yoon, S.J. Lee, M. Narumiya, N. Nakada, I.S. Han, H. Tanaka, Occurrence and Fate of PPCPs Wastewater Treatment Plants in Korea, Vol. 35, 2nd International Conference on Environment and Industrial Innovation, IPCBEE, IACSIT Press, Singapore, 2012, pp. 57–61.
[50] M.F. Mohd Amin, S.G.J. Heijman, L.C. Rietveld, Clay–starch combination for micropollutants removal from wastewater treatment plant effluent, Water Sci. Technol., 73 (2016) 1719–1727.
[51] M. Anis, S. Haydar, Heterogeneous Fenton oxidation of caffeine using zeolite-supported iron nanoparticles, Arabian J. Sci. Eng., 44 (2019) 315–328.
[52] H. Tamura, K. Goto, T. Yotsuyanagi, M. Nagayama, Spectrophotometric determination of iron(II) with 1,10-phenanthroline in the presence of large amounts of iron(III), Talanta, 21 (1974) 314–318.
[53] S. Ranga, M. Jaimini, S.K. Sharma, B.S. Chauhan, A. Kumar, A review on Design of Experiments (DOE), Int. J. Pharm. Chem. Sci., 3 (2014) 216–224.
[54] J. Virkutyte, E. Rokhina, V. Jegatheesan, Optimisation of electro-Fenton denitrification of a model wastewater using a response surface methodology, Bioresour. Technol., 101 (2010) 1440–1446.
[55] A.G. Trovó, T.F.S. Silva, O. Gomes Jr., A.E. Machado, W.B. Neto, P.S. Muller Jr., D. Daniel, Degradation of caffeine by photo-Fenton process: optimization of treatment conditions using experimental design, Chemosphere, 90 (2013) 170–175.
[56] M. Ahmadi, F. Ghanbari, S.M. Bidgoli, Photoperoxi-coagulation using activated carbon fiber cathode as an efficient method for benzotriazole removal from aqueous solutions: modeling, optimization and mechanism, J. Photochem. Photobiol., A, 322–323 (2016) 85–94.
[57] P. Cañizares, R. Paz, C. Sáez, M.A. Rodrigo, Costs of the electrochemical oxidation of wastewaters: a comparison with ozonation and Fenton oxidation processes, J. Environ. Manage., 90 (2009) 410–420.